

## Does the $1/f$ frequency-scaling of brain signals reflect self-organized critical states ?

C. Bédard<sup>a,b</sup>, H. Kröger<sup>b</sup>, A. Destexhe<sup>a,\*</sup>

<sup>a</sup> Integrative and Computational Neuroscience Unit (UNIC),

CNRS, Gif-sur-Yvette, France

<sup>b</sup> Department of Physics,

Université Laval, Québec, Canada

\* Corresponding Author, [destexhe@iaf.cnrs-gif.fr](mailto:destexhe@iaf.cnrs-gif.fr)

(Dated: October 24, 2018)

Many complex systems display self-organized critical states characterized by  $1/f$  frequency scaling of power spectra. Global variables such as the electroencephalogram, scale as  $1/f$ , which could be the sign of self-organized critical states in neuronal activity. By analyzing simultaneous recordings of global and neuronal activities, we confirm the  $1/f$  scaling of global variables for selected frequency bands, but show that neuronal activity is not consistent with critical states. We propose a model of  $1/f$  scaling which does not rely on critical states, and which is testable experimentally.

PACS numbers: 87.19.Nn, 89.75.Da, 02.50.Ey, 05.40.-a, 87.18.-h

Self-organized critical states are found for many complex systems in nature, from earthquakes to avalanches [1, 2]. Such systems are characterized by scale invariance, which is usually identified as a power-law distribution of variables such as event duration or the waiting time between events.  $1/f$  noise is usually considered as a footprint of such systems [1].  $1/f$  frequency scaling is interesting, because it betrays long-lasting correlations in the system, similar to the behavior near critical points.

Several lines of evidence point to the existence of such critical states in brain activity. Global variables, such as the electroencephalogram (EEG) and magnetoencephalogram, display frequency scaling close to  $1/f$  [3, 4]. EEG analysis [5] and avalanche analysis of local field potentials (LFPs) recorded *in vitro* [6] provided clear evidence for self-organized critical states with power-law distributions. There is also evidence for critical states from the power-law scaling of interspike interval (ISI) distributions computed from retinal, visual thalamus and primary visual cortex neurons [7]. In addition, model networks of neurons indicate that critical states may be associated with frequency scaling consistent with experiments [8]. However, these are independent evidences from different preparations and the link between  $1/f$  frequency scaling of global variables and the existence of critical states in neural activity has not been firmly established. Moreover,  $1/f$  spectra are not necessarily associated with critical states [9], so it is not clear if the intact and functioning brain operates in a

way similar to critical states.

To attempt answering these questions, we first investigated if  $1/f$  frequency scaling is present in global variables recorded close to the underlying neuronal current sources *in vivo*. We analyzed cortical LFPs which were recorded within cerebral cortex using bipolar extracellular high-impedance microelectrodes [10]. Bipolar LFP recordings sample relatively localized populations of neurons, as these signals can be very different for electrodes separated by 1 mm apart [10]. This stands in contrast with the EEG, which samples much larger populations of neurons [11] and is recorded from the surface of the scalp using millimeter-scale electrodes. LFPs are subject to much less filtering compared to EEG, because EEG signals must diffuse through various media, such as cerebrospinal fluid, dura matter, cranium, muscle and skin. Thus, finding  $1/f$  frequency scaling of bipolar LFPs would be a much stronger evidence that this scaling reflects neuronal activities, as these signals are directly recorded from within the neuronal tissue. Moreover, in order to distinguish state-dependent scaling properties, we have compared recordings during wakefulness and slow-wave sleep in the same experiments.

Bipolar LFPs from cat parietal association cortex show the classic landmarks of EEG signals in these states [12], namely during waking, LFPs are of low amplitude and very irregular (Fig. 1, top trace), and are dominated by beta frequencies (around 20 Hz). This pattern is also called “desynchronized” activity, and is typically seen during aroused states in the hu-

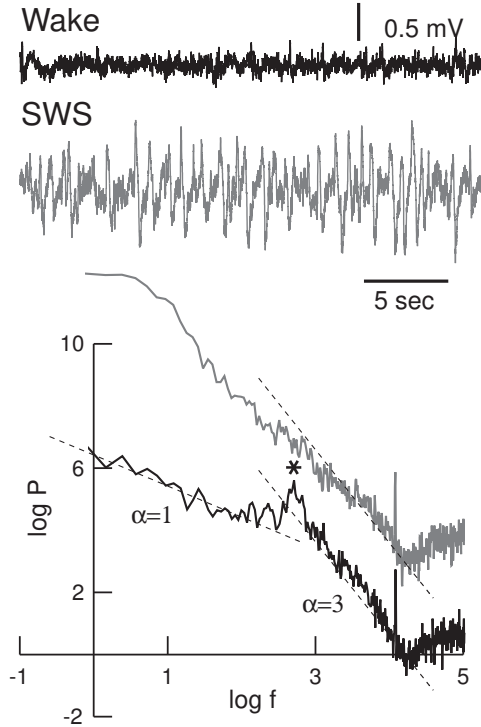


FIG. 1: Frequency scaling of local field potentials from cat parietal cortex. Top traces: LFPs recorded in cat parietal cortex during wake and slow-wave sleep (SWS) states. Bottom: Power spectral density of LFPs, calculated from 55 sec sampled at 300 Hz (150 Hz 4th-order low-pass filter), and represented in log-log scale (dashed lines represent  $1/f^\alpha$  scaling). During waking (black), the frequency band below 20 Hz scales approximately as  $1/f$  (\*: peak at 20 Hz beta frequency), whereas the frequency band between 20 and 65 Hz scales approximately as  $1/f^3$ . During slow-wave sleep (gray; displaced upwards), the power in the slow frequency band is increased, and the  $1/f$  scaling is no longer visible, but the  $1/f^3$  scaling at high frequencies remains unaffected. PSDs were calculated over successive epochs of 32 sec, which were averaged over a total period of 200 sec for Wake and 500 sec for SWS.

man EEG [11]. During slow-wave sleep, LFPs display high-amplitude slow-wave activity (Fig. 1, middle trace), similar to the “delta waves” of human sleep EEG [11]. The power spectral density (PSD) calculated from these LFPs typically shows a broad-band structure. During wakefulness, the PSD shows two different scaling regions, according to the frequency band. For low frequencies (between 1 and 20 Hz), the PSD scales approximately as  $1/f$ , whereas for higher frequencies

(between 20 and 65 Hz), the scaling is approximately of  $1/f^3$  (Fig. 1, black PSD). During slow-wave sleep, the additional power at slow frequencies masks the  $1/f$  scaling, but the same  $1/f^3$  scaling is present in the high-frequency band (Fig. 1, gray PSD). The same behavior was observed for other electrodes in the same experiment, and in three other animals (not shown). Thus, these results confirm that the  $1/f$  frequency scaling reported in the EEG [3] is also present in bipolar LFPs from cat association cortex, but only during waking and for specific frequency bands.

To investigate whether this  $1/f$  scaling is associated with self-organized critical states, we first analyzed the ISI distributions from neurons recorded in cat parietal cortex. Unit activity was recorded simultaneously with LFPs at 8 locations separated by 1 mm [10]. The distribution of ISIs was computed for individual neurons, and were represented in log-linear scale (Fig. 2; log-log scale in insets). For both wakefulness and slow-wave sleep (Fig. 2A and B), the distributions showed no evidence for power law behavior. During waking, the ISI distributions were close to exponentially-distributed ISIs, as generated by Poisson stochastic process with same statistics as the neurons analyzed (Fig. 2, Poisson). For 22 neurons recorded during the wake state, the Pearson coefficient was of  $0.91 \pm 0.13$  for exponential distribution fits, and of  $0.86 \pm 0.16$  for power-law distribution fits. Taking only the subset of 7 neurons with more than 2000 spikes, the fit was nearly perfect for exponential distributions (Pearson coefficient of  $0.999 \pm 0.001$ ). However, during slow-wave sleep, there was a marked difference between the experimental ISI and the corresponding Poisson process (Fig. 2B). In this state, neurons tended to produce long periods of silences, which are related to EEG slow waves [10, 12], and which is visible as a prominent tail of the distribution for large ISIs. This tail was well fit by a Poisson process of low rate (Fig. 2B, dashed line).

To further check for criticality, we have performed an avalanche analysis by taking into account the collective information from the multisite recordings. We used the same method as for ref. [6], which amounts to detect clusters of contiguous events separated by silences, by binning the system in time windows of 1 ms to 16 ms [6]. As there was no evidence for any recognizable event in LFPs which could be taken as avalanche (see Fig. 1), we used the spike times among the ensemble of simultaneously recorded neurons. The distribution of avalanche size does not follow power-law

scaling (Fig. 2C, black), but is closer to an exponential distribution as predicted by Poisson processes (Fig. 2C, gray). This analysis therefore confirms the absence of avalanche dynamics in this system [16].

To explain the  $1/f$  scaling of LFPs, we attempted to reconstruct LFPs from unit activity. Unit activity is displayed in Fig. 3 (top) for the same experiment as that of Fig. 1. Because LFPs are generated primarily by synaptic currents in neurons [11, 13], and because synaptic currents are very well modeled by simple exponential relaxation processes [14], we modeled the synaptic current from the following convolution [15]:

$$C(t) = \int_{-\infty}^{\infty} D(t') \exp[-(t-t')/\tau_s] dt', \quad (1)$$

where  $C(t)$  is the synaptic current and  $D(t)$  is the “drive” signal which consisted in the experimentally-recorded spike trains. The PSD of the synaptic current is then given by:

$$S(\omega) = |C(\omega)|^2 = \frac{|D(\omega)|^2}{1 + \omega^2 \tau_s^2}. \quad (2)$$

The PSD of synaptic currents reconstructed from experimentally-recorded spikes showed an approximate Lorentzian behavior ( $1/f^2$  scaling) during wakefulness (Fig. 3, Wake), as expected from the exponential nature of synaptic events. During slow-wave sleep, there was more power for slow frequencies, but the  $1/f^2$  scaling at high frequencies was still present (Fig. 3, SWS). The Lorentzian form of the PSD in Fig. 3 (Wake) shows that in the waking state,  $|D(\omega)|^2$  is approximately constant, therefore the drive  $D(t)$  is statistically equivalent to a white noise process, consistent with the apparent Poisson statistics of spikes identified in Fig. 2 (see also refs. [17] for similar findings in awake monkeys). During slow-wave sleep, however, the deviation from the Lorentzian suggests that  $D(t)$  is a stochastic process statistically different from white noise, and contains in addition increased power at low frequencies, also consistent with the analysis of Fig. 2.

This model, however, does not yield PSD consistent with the  $1/f$  and  $1/f^3$  scaling of LFPs shown in Fig. 1. Interestingly, the scaling of this model is in  $1/f^0$  or  $1/f^2$  for the same frequency bands that displayed  $1/f$  or  $1/f^3$  in LFPs, respectively. Using a similar convolution equation to model the PSD of LFPs

$$LFP(t) = \int_{-\infty}^{\infty} C(t') F(t-t') dt', \quad (3)$$

where  $C(t)$  is the synaptic current source and  $F(t)$  is a function representing a filter. As above, the PSD is given by

$$P(\omega) = |LFP(\omega)|^2 = |C(\omega)|^2 |F(\omega)|^2. \quad (4)$$

In this model, the frequency scaling of the PSD of both wakefulness and slow-wave sleep LFPs in Fig. 1 can be explained by assuming that the filter scales as  $1/f$ , or equivalently that  $|F(\omega)|^2 \sim 1/\omega$ . In other words, this model can explain qualitatively the  $1/f$  and  $1/f^3$  scaling of LFPs under the condition that neuronal current sources are subject to an  $1/f$  filter. Such a filter is most likely due to the filtering of extracellular currents through the tissue, before it reaches the electrode [18].

Finally, we provide an intuitive justification for this predicted  $1/f$  filter, as well as possible ways to test it experimentally. The  $1/f$  filtering of extracellular media can be justified intuitively by considering the complex structure of such media, and in particular its spatial irregularity. Extracellular space consists of a complex arrangement of cellular processes of various size and irregular shape, while the extracellular fluid represents only a few percent of the available space [19]. The effect of a current source in such media will be a combination of resistive effects, due to the flow of current in the conductive fluids, and capacitive effects, due to the high density of membranes (for a theoretical treatment see refs. [18]). Such a complex arrangement of resistors and capacitors with random values is known to produce an  $1/f$  filter, as found for inhomogeneous materials [20]. Although such materials are different from the structure of biological media, it is plausible that similar considerations may explain the  $1/f$  filtering predicted here. Linear arrangements of RC circuits with random values (RC line) also generates  $1/f$  noise [21]. Superposition of a large number of exponential relaxation processes with different relaxation rates can also generate  $1/f$  scaling [22, 23]. Understanding of the  $1/f$  filtering by extracellular media based on plausible biophysical models is presently under investigation. The predicted  $1/f$  filter could also be tested experimentally by injecting white noise currents (of amplitude comparable to neuronal current sources) in extracellular space, and measuring the resulting field potential at some distance from the injection site. This measured LFP should scale as  $1/f$ .

In conclusion, we have shown that the PSD of bipo-

lar LFPs from cat parietal cortex displays several scaling regions, as  $1/f$  or  $1/f^3$  depending on the frequency band and behavioral state. By analyzing neuronal unit activity from the same experiments, we did not see evidence that this  $1/f$  scaling is associated with critical states. Neither ISI distributions nor avalanche size distributions display power-law scaling, but are rather consistent with Poisson processes. We provided an alternative explanation for  $1/f$  frequency scaling which does not rely on critical states, but rather stems from the filtering properties of extracellular media. We gave an intuitive explanation for a possible physical origin of such  $1/f$  filtering, as well as a way to test it experimentally. These results may appear to contradict with previous evidence for critical states in vitro [6] or in the early visual system in vivo [7]. However, the absence of critical states reported here may instead reflect fundamental differences between association cortex and other structures more directly related to sensory inputs. Future work should clarify why different structures show different scaling, and what implications it may have for brain dynamics and coding.

The experimental data analyzed in this article were obtained with Drs. Diego Contreras and Mircea Steriade, and were published previously [10]. We are grateful for support by NSERC Canada (H.K.), CNRS, the European Commission (FET program), and the HFSP program (A.D.).

- 
- [1] H.J. Jensen, *Self-Organized Criticality. Emergent Complex Behavior in Physical and Biological Systems*. (Cambridge University Press, Cambridge UK, 1998).
- [2] P. Bak, *How Nature Works* (Springer-Verlag, New York, 1996).
- [3] W.S. Pritchard, *Int. J. Neurosci.*, **66**, 119 (1992); W.J. Freeman, L.J. Rogers, M.D. Holmes & D.L. Silbergeld, *J. Neurosci. Methods* **95**, 111 (2000); P.A. Robinson, C.J. Rennie, J.J. Wright, H. Bahramali, E. Gordon, D.L. Rowe, *Phys. Rev. E* **63**, 021903 (2001).
- [4] E. Novikov, A. Novikov, D. Shannahoff-Khalsa, B. Schwartz, J. Wright, *Phys. Rev. E* **56**, R2387 (1997).
- [5] K. Linkenkaer-Hansen, V.V. Nikouline, J.M. Palva & R.J. Ilmoniemi, *J. Neurosci.* **21**, 1370 (2001); W.J. Freeman, M.D. Holmes, G.A. West & S. Vanhatalo, *Clin. Neurophysiol.* **117**, 1228 (2006).
- [6] J. Beggs, D. Plenz, *J. Neurosci.* **23**, 11167 (2003).
- [7] M.C. Teich, C. Heneghan, S.B. Lowen, T. Ozaki & E. Kaplan, *J. Opt. Soc. Am. A* **14**, 529 (1997); A.R.R. Papa, L. da Silva, *Theory in Biosciences* **116**, 321 (1997).
- [8] L. de Arcangelis, C. Perrone-Capano, H.J. Herrmann, *Phys. Rev. Lett.* **96**, 028107 (2006).
- [9] P. De Los Rios, Y.C. Zhang, *Phys. Rev. Lett.* **82**, 472 (1999); T. Giesinger, *Biol. Rev.* **76**, 161 (2001).
- [10] A. Destexhe, D. Contreras, M. Steriade, *J. Neurosci.* **19**, 4595 (1999).
- [11] E. Niedermeyer, F. Lopes da Silva, (editors) *Electroencephalography* (Williams & Wilkins, Baltimore MD 1998).
- [12] M. Steriade, *Neuronal Substrates of Sleep and Epilepsy* (Cambridge University Press, Cambridge UK, 2003).
- [13] P.L. Nunez, *Electric Fields in the Brain. The Neurophysics of EEG* (Oxford University Press, Oxford UK, 1981).
- [14] A. Destexhe, Z. Mainen, T.J. Sejnowski, In: *Methods in Neuronal Modeling* (C. Koch, I. Segev, eds; MIT Press, Cambridge MA, 1998), pp. 1-26.
- [15] Nearly identical results were obtained using a biophysical model based on a passive membrane equation where experimentally-recorded spikes triggered conductance-based synaptic inputs.
- [16] A complete demonstration of the absence of critical states would require investigating other dynamical features, such as long-lived metastable states; see M. Paczuski, P. Bak, S. Maslov, *Phys. Rev. E* **53**, 414 (1996).
- [17] W.R. Softky, C. Koch, *J. Neurosci.* **13**, 334 (1993); W. Bair, C. Koch, W. Newsome & K. Britten, *J. Neurosci.* **14**, 2870 (1994).
- [18] C. Bedard, H. Kröger, A. Destexhe, *Biophys. J.* **86**, 1829 (2004); C. Bedard, H. Kröger, A. Destexhe, *Phys. Rev. E* **73**, 051911 (2006).
- [19] A. Peters, S.L. Palay, H.F. Webster, *The Fine Structure of the Nervous System* (Oxford University Press, Oxford UK, 1991).
- [20] D.P. Almond, B. Vainas, *J. Phys.: Condens. Matter* **13**, L361 (2001).
- [21] A.A. Verveen, L.J. DeFelice, *Prog. Biophys. Mol. Biol.* **28**, 189 (1974).
- [22] J. Bernamont, *Ann. Physique* **7**, 71 (1937); R.B. Anderson, *Mem. Cognit.* **29**, 1061 (2001).
- [23] This mechanism is however not plausible, because it would require a uniform distribution of decay times of synaptic currents across a large range of values, whereas only a few receptor types are present in biological tissue, with well-defined decay times.

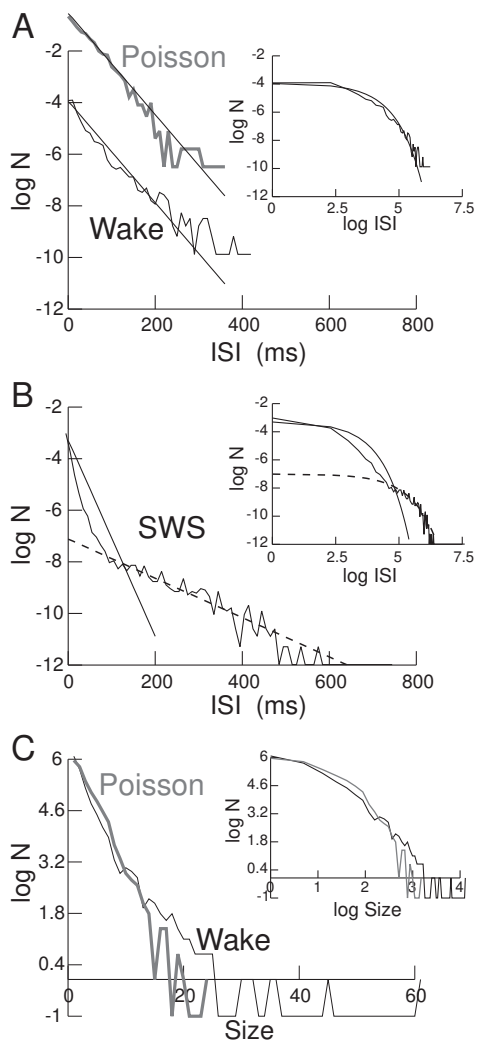


FIG. 2: Absence of power law distributions in neuronal activity. The logarithm of the distribution of interspike intervals (ISI) during waking (Wake, A, 1951 spikes) and slow-wave sleep (SWS, B, 15997 spikes) is plotted as a function of ISI length, or  $\log$  ISI length (insets). A Poisson process of the same rate and statistics is displayed in A (Poisson; gray curve displaced upwards for clarity). The exponential ISI distribution predicted by Poisson processes of equivalent rates is shown as straight lines (smooth curve in inset). The dotted line in B indicates a Poisson process with lower rate which fits the tail of the ISI distribution in SWS. C. Avalanche analysis realized by taking into account the statistics from all simultaneously-recorded cells in Wake. The distribution of avalanche sizes scales exponentially (black curves), similar to the same analysis performed on a Poisson process with same statistics (gray curves).

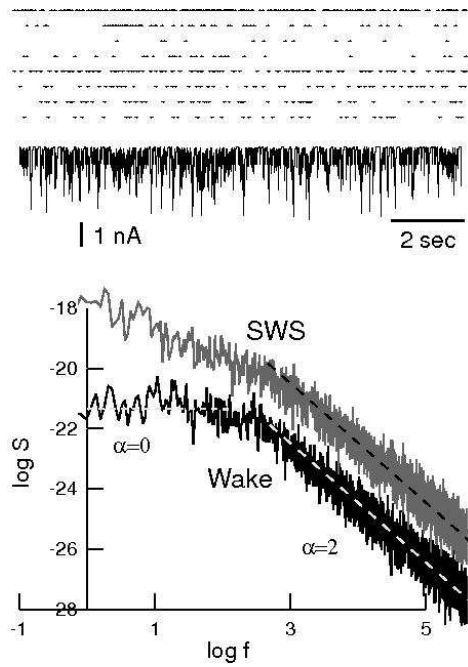


FIG. 3: Frequency scaling of synaptic currents reconstructed from spike times. Top traces: raster plot of spiking times of 8 multi-unit recordings in cat cortex during wakefulness (same experiment as in Fig. 1; data from ref. [10]). Middle trace: total synaptic current obtained by convolving the spike times with exponential relaxation processes ( $\tau_s=10$  ms). Bottom: PSD of synaptic currents for wake (black) and slow-wave sleep (SWS; PSD in gray displaced upwards for clarity); dashed lines represent  $1/f^\alpha$  scaling.